



HAL
open science

INDENTATION OF AN ELASTIC HALF SPACE

Jacques Woirgard

► **To cite this version:**

Jacques Woirgard. INDENTATION OF AN ELASTIC HALF SPACE. Philosophical Magazine, 2006, 86 (33-35), pp.5199-5217. 10.1080/14786430600651970 . hal-00513680

HAL Id: hal-00513680

<https://hal.science/hal-00513680>

Submitted on 1 Sep 2010

HAL is a multi-disciplinary open access archive for the deposit and dissemination of scientific research documents, whether they are published or not. The documents may come from teaching and research institutions in France or abroad, or from public or private research centers.

L'archive ouverte pluridisciplinaire **HAL**, est destinée au dépôt et à la diffusion de documents scientifiques de niveau recherche, publiés ou non, émanant des établissements d'enseignement et de recherche français ou étrangers, des laboratoires publics ou privés.



INDENTATION OF AN ELASTIC HALF SPACE

Journal:	<i>Philosophical Magazine & Philosophical Magazine Letters</i>
Manuscript ID:	TPHM-05-Nov-0506.R2
Journal Selection:	Philosophical Magazine
Date Submitted by the Author:	17-Feb-2006
Complete List of Authors:	Woïrgard, Jacques; CNRS
Keywords:	indentation, contact mechanics, elasticity
Keywords (user supplied):	adhesion, contact area, indentation



Only

ABSTRACT

This paper presents some results on the indentation of an elastic half space. In the first part an approximate analytical expression is proposed for the stress distribution on a half space under a flat punch with a cross sections in the form of a regular polygon. Accurate values for the beta parameter are computed for triangular and square cross sections. These values, corresponding for example to Berkovich and Vickers indenters, are respectively 1.06142 and 1.02121.

In a second part, the influence of radial displacements on the β parameter is examined according to a previous idea of Bolshakov and Pharr. An alternative expression for this parameter is proposed giving lower values than those proposed by these authors. Since in most elastoplastic materials the equivalent indenters used during unloading are in the form of paraboloids rather than cones, as in the well known method of Oliver and Pharr, this case is examined in details. A simple formula is also proposed for the the radial displacements in the case of indenters described by polynomials or obeying power laws with non integer exponents. The conclusions concerning equivalent indenters in the form of paraboloids are then compared with preliminary experimental results obtained with a new indenter made of a cube-corner terminated by a Berkovich part. This indenter and another prismatic one allow a direct determination of the contact area eliminating uncertainties due to the presence of pile-up or sinking-in.

Beta: Indentation: Elasticity

SOME RESULTS ON THE INDENTATION OF AN ELASTIC HALF SPACE

Jacques Woirgard

**Laboratoire de Métallurgie Physique
Université de Poitiers SP2MI
UMR CNRS 6630
86962 Futuroscope-Chasseneuil
France**

For Peer Review Only

1
2
3
4
5
6
7
8
9
10
11
12
13
14
15
16
17
18
19
20
21
22
23
24
25
26
27
28
29
30
31
32
33
34
35
36
37
38
39
40
41
42
43
44
45
46
47
48
49
50
51
52
53
54
55
56
57
58
59
60

1 INTRODUCTION

With some assumptions instrumented indentation tests make possible the determination of mechanical parameters such as the hardness and the elastic modulus of materials. Analysis of experimental data requires a precise knowledge of the projected contact area under load. Since classical indentation tests do not give directly this essential parameter various models have been proposed to derive this contact area from experimental data. These data consist mainly in the applied load, the total penetration depth and the sample stiffness. This stiffness is deduced either from unloading curves or obtained continuously during loading and unloading [1]. The stiffness is then used through different models [2], [3], [4] [5], to estimate the contact area under load. The accuracy of these calculations is relatively poor especially when surface deformations like pile-up or sinking-in occur. It is one of the reasons why a new experimental method allowing a direct determination of this important parameter will be briefly presented at the end of the paper.

Once the contact area is known, the Meyer hardness H (mean contact pressure) is given by:

$$H = \frac{F}{A}$$

where A is the projected contact area, S the stiffness and F the applied load. The Young's modulus E can be deduced from the following equation, ν being the Poisson's ratio:

$$S = \frac{2}{\sqrt{\pi}} \frac{E}{1-\nu^2} \sqrt{A}$$

The formula is frequently credited to Sneddon but it was first proposed by Bulishev, Alekhin and Shorshorov [6] and will be referred to as the BASH formula.

However the formula corresponds to small deformations of an elastic half plane by an axisymmetric frictionless punch and is no more valid when the contact is not entirely frictionless and (or) the punch is not axisymmetric as most real indenters like Vickers, Berkovich or cube corners.

To make the BASH formula more precise it is often proposed to introduce an additional parameter β [3], [7].

$$S = \beta \frac{2}{\sqrt{\pi}} \frac{E}{1-\nu^2} \sqrt{A}$$

One of the aim of this paper is first to contribute to a precise evaluation of the β parameter and in a second part to present some results concerning the evaluation of normal stresses and radial displacements.

2 CORRECTIONS FOR NON AXISYMMETRIC PUNCHES

The problem of determining the pressure distribution on the surface of an elastic half plane under a frictionless flat punch of arbitrary shape submitted to a force applied at the centre of gravity is important for indentation experiments. Regarding the medium as isotropic and neglecting friction forces, the elastic compliance for tips of any shapes can be calculated thanks to Betti's [8] reciprocal theorem, once the pressure distribution for the flat punch of same cross section is known.

The solution of the problem requires solving the first kind Fredholm integral equation associated with the corresponding boundary value problem. A similar equation is encountered in other branches of physics. For example in electrostatics for the determination of the capacitance of a single charged conducting surface, the density of charges corresponding to the pressure distribution for an elastic

contact. Unfortunately exact analytical solutions can only be found for some simple geometries as circular or elliptical ones. A lot of numerical methods have been proposed to solve the integral equation [8], [9], [10]. These methods suffer when the boundary presents sharp corners, as for example polygons, since the corresponding density goes rapidly to infinity at the corners. Another inconvenience is that numerical methods do not give analytical expressions for the density.

Another approach consists in finding some trial function approximating the desired density, see for example [11], [12]. One of the purposes of this paper is then to propose a general analytical expression giving an acceptable approximation for the density in the case of regular polygons. For domains in the form of equilateral triangles or squares, corresponding respectively to Berkovich and Vickers indenters, slightly modified expressions leading to a much better approximations will be proposed.

2-1 Theory

A unit source located at a point \mathbf{q} generates the Newtonian potential $V(\mathbf{p})$, at the point \mathbf{p} , $d(\mathbf{p},\mathbf{q})$ being the distance between points \mathbf{p} and \mathbf{q} . For example a continuous density distribution $\sigma(\mathbf{q})$ of sources over a plane domain \mathbf{B} generates the potential:

$$V(\mathbf{p}) = \iint_{\mathbf{B}} \sigma(\mathbf{q}) d(\mathbf{p},\mathbf{q})^{-1} d\mathbf{q}$$

The case of a constant potential $V(\mathbf{p})$ over the domain corresponds for example to the calculation of the capacitance of a single charged conducting surface or, in elasticity, to the pressure distribution under a flat indenter. In this case the uniform displacement of the surface is given by:

$$u(\mathbf{p}) = \frac{1-\nu^2}{\pi E} V(\mathbf{p})$$

For circular or elliptical domains exact solutions are known.

For a circle the pressure distribution varies as:

$$\sigma_c = \left(1 - \frac{x^2 + y^2}{R^2}\right)^{-\frac{1}{2}}$$

and for an ellipse with semi-axis a and b :

$$\sigma_e = \left(1 - \left(\frac{x^2}{a^2} + \frac{y^2}{b^2}\right)\right)^{-\frac{1}{2}}$$

In both cases the pressure goes to infinity on the boundary. For a regular polygon, it is possible to divide the domain in elementary triangles and limit the calculation of the density to one of this triangles as shown in Figure 1. The coordinates of the point \mathbf{p} belonging to such a triangle are taken as \mathbf{a} and $\mathbf{v}=\tan\theta$. The simplest form of the density σ can being:

$$\sigma = (1 - a^2)^{-\frac{1}{2}} \quad (1)$$

Such an expression, analogue to that proposed by Fabrikant [12], may be acceptable for smooth boundaries but certainly not for polygons with sharp corners. Indeed it has been shown [13] that the density at a point \mathbf{q} in the neighbourhood of a non singular point \mathbf{p} of the boundary varies as: $d(\mathbf{p},\mathbf{q})^{-1}$ and goes more rapidly to infinity close to a corner [14].

The potential corresponding to Fabrikant's formula, i.e. to equation (1) cannot be regarded as constant since it varies of as much as 28% for the equilateral triangle and 18% for the square, which is hardly acceptable. So it seems necessary to introduce some corrections to take into account the rapid increase of the density in the neighbourhood of the corners.

For a domain presenting some symmetry, as for example a regular polygon, the density has only to be calculated in an elementary triangle as shown in figure (2), the integration for the potential calculation being extended to the whole domain. The general expression proposed to approximate the density is:

$$\sigma = (1-a^2)^{-\frac{1}{2}} \left\{ \prod_i \left[(x_i - a)^2 + \left(\frac{y_i}{x_i} - v \right)^2 \right] \right\}^{-\frac{1}{2n+1}}$$

for a regular polygon with n summits of coordinates x_i , y_i , \mathbf{a} varying for the sake of simplicity, between 0 and 1.

The expression becomes for an equilateral triangle:

$$\sigma = (1-a^2)^{-\frac{1}{2}} \left\{ [(1-a)^2 + (\sqrt{3}-v)^2] [(1-a)^2 + (\sqrt{3}+v)^2] [(2+a)^2 + v^2] \right\}^{-\frac{1}{7}}$$

and for a square:

$$\sigma = (1-a^2)^{-\frac{1}{2}} \left\{ [(1-a)^2 + (1-v)^2] [(1-a)^2 + (1+v)^2] [(1+a)^2 + (1-v)^2] [(1+a)^2 + (1+v)^2] \right\}^{-\frac{1}{9}} \quad (2)$$

The corresponding potential variations are 2.9% for the triangle, 1.1% for the square and 1.0% for the hexagon. It can be seen that the precision increases with the number of corners, the extreme case being the circle where this number goes to infinity, and the corresponding exponent to zero.

To check the validity of the proposed density we can compute the value of the capacitance of a single charged square plate. Equation (2) gives:

$$C=0.3676$$

very close to the value proposed by Noble [9]:

$$C=0.367$$

The value found by Fabrikant[12] was slightly different:

$$C=0.3611.$$

For the penetration of the flat punch, equations (1 and 2) lead to mean values for the correction factor β :

$$\beta= 1.061$$

for the equilateral triangle and

$$\beta= 1.023$$

for the square (Vickers indenter).

The value obtained for the triangle is larger than previously proposed ones [13], [14], [15].

2-2 Modified solutions for the equilateral triangle and the square

More precise expressions for the equilateral triangle and the square can be proposed corresponding to the most commonly used indenters: Berkovich or cube-corner for the triangle and Vickers for the square. These solutions, obtained by slightly modifying the general expressions, cannot be extended to other indenters. However, if necessary, it would be certainly possible to do the same kind of optimisation for other geometries. The proposed modified densities are:

$$\sigma = (1-a^2)^{-0.4966} \left\{ [(1-a)^2 + 1.17(\sqrt{3}-v)^2] [(1-a)^2 + 1.23(\sqrt{3}+v)^2] [(2+a)^2 + 0.72v^2] \right\}^{-0.1354}$$

for the triangle and

$$\sigma = (1-a^2)^{-\frac{1}{2}} \left\{ [(1-a)^2 + 2.3(1-v)^2] [(1-a)^2 + (1+v)^2] [(1+a)^2 + 1.8(1-v)^2] [(1+a)^2 + (1+v)^2] \right\}^{-0.1055}$$

for the square.

When the integration is extended to the whole domain x varying between 0 and 0.99, the potential

variations around the mean value are less than 0.30% for the triangle and 0.39% for the square. The corresponding β values being respectively:

$$\begin{aligned}\beta &= 1.0614 && \text{for the triangle and} \\ \beta &= 1.022 && \text{for the square.}\end{aligned}$$

To still improve the accuracy in these cases of practical interest, further corrections in the form of polynomials in both \mathbf{a} and \mathbf{v} have been introduced, minimizing the root mean square error. With these corrections potential variations are less than 10^{-5} , giving final β values

$$\begin{aligned}\beta &= 1.06142 && \text{for the triangle} \\ \text{and} \\ \beta &= 1.02121 && \text{for the square.}\end{aligned}$$

As regards the capacitance of the square, for which some results are available in the literature [8], [9], it was found:

$$C = 0.36768.$$

Then it appears that relatively simple approximate analytical expressions for the density, or the pressure distribution, can be used, with an accuracy comparing favourably to numerical methods.

3 INFLUENCE OF THE RADIAL DISPLACEMENTS

As first mentioned by Bolshakov and Pharr [18], applying Sneddon's equilibrium equations [19] for the indentation of an elastic half plane by a frictionless axisymmetric rigid indenter, leads to a surface deformation not fitting the indenter shape. This happens when radial displacements are taken into account. Thus, to insure that the surface deformation exactly fits the indenter shape the authors proposed as the exact solution of the problem to use the following relationship, with Θ the indenter included half angle:

$$w(\rho) + \frac{1}{\tan \theta} u(\rho) = D - f(\rho) \quad \rho < a$$

For a cone this equation is equivalent to:

$$w(\rho) = D - f(\rho + u(\rho)) \quad (3)$$

which is only a first order approximation for other geometries of indenters. In these equations $\rho = r/a$, a being the contact radius, $w(\rho) = u_z(\rho)$ the normal displacement and $f(\rho)$ a function fitting the indenter shape.

Using Sneddon's results and Busbridge equation [20] [21], the authors claimed that $u(\rho)$ is the solution of the following equation:

$$u = \frac{1-2\nu}{4(1-\nu)} \frac{\cot \theta}{\pi} \left(\frac{\pi}{4} \rho \ln \frac{\rho}{1+\sqrt{1-\rho^2}} - \frac{\pi}{4} \frac{1-\sqrt{1-\rho^2}}{\rho} + \frac{1}{\rho} \int_0^1 \frac{yu(y)dy}{\sqrt{1-y^2}} - \frac{1}{\rho} \int_1^\rho \frac{x^2 dx}{\sqrt{x^2-\rho^2}} \int_0^x \frac{du/dy}{\sqrt{x^2-y^2}} dy \right)$$

However since this equation is not very tractable an approximate solution [22] was proposed leading to the following value for the β parameter:

$$\beta = \pi \frac{\frac{\pi}{4} + 0.15483073 \frac{1-2\nu}{4(1-\nu)} \cot \theta}{\left(\frac{\pi}{2} - 0.83119312 \frac{1-2\nu}{4(1-\nu)} \cot \theta \right)^2} \quad (4)$$

To obtain this result the authors proposed to modify the shape of the indenter, i.e. the stress distribution, insuring that the surface deformation exactly fits the shape of the original indenter.

However, when strictly applying Sneddon's equations, a different result is obtained as shown below.

The normal displacement $w(\rho)$ can be written taking into account the radial displacements and using equation (3) as a first order approximation:

$$w(\rho) = D - a \cot \theta \left[\rho + \frac{1-2\nu}{4(1-\nu)} \rho \cot \theta \left(\text{Log} \frac{\rho}{1+\sqrt{1-\rho^2}} - \frac{1-\sqrt{1-\rho^2}}{\rho^2} \right) \right]$$

Using Sneddon results [23] with:

$$f(\rho) = a \cot \theta \left(\rho + \frac{1-2\nu}{4(1-\nu)} \rho \cot \theta \left(\text{Log} \frac{\rho}{1+\sqrt{1-\rho^2}} - \frac{1-\sqrt{1-\rho^2}}{\rho^2} \right) \right)$$

the total penetration D and the load P can be calculated:

$$D = \int_0^1 \frac{f'(\rho) d\rho}{\sqrt{1-\rho^2}}$$

and:

$$P = \int_0^1 \frac{\rho^2 f'(\rho) d\rho}{\sqrt{1-\rho^2}}$$

After evaluating numerically the integrals one gets for the penetration:

$$D = a \cot \theta \left[\frac{\pi}{2} - 0.83193 \frac{1-2\nu}{4(1-\nu)} \cot \theta \right]$$

for the load:

$$P = 2a^2 \frac{E}{1-\nu^2} \cot \theta \left[\frac{\pi}{4} + 0.15483 \frac{1-2\nu}{4(1-\nu)} \cot \theta \right]$$

And for the stiffness S :

$$S = \frac{dP}{dD} = \frac{dP}{da} / \frac{dD}{da} = 4a \frac{E}{1-\nu^2} \frac{\cot \theta \left[\frac{\pi}{4} + 0.15483 \frac{1-2\nu}{4(1-\nu)} \cot \theta \right]}{\cot \theta \left[\frac{\pi}{2} - 0.83193 \frac{1-2\nu}{4(1-\nu)} \cot \theta \right]}$$

The corresponding β value being:

$$\beta = 2 \frac{\frac{\pi}{4} + 0.15483 \frac{1-2\nu}{4(1-\nu)} \cot \theta}{\frac{\pi}{2} - 0.83193 \frac{1-2\nu}{4(1-\nu)} \cot \theta} \quad (5)$$

This result differs from that given in reference [22] by a factor

$$\frac{\pi D}{2 a}$$

equals to 1 to 1 for a cone. However the origin of this factor is not clearly explained in [22].

For $\nu=0$ and a cube-corner with an equivalent angle of 42.3° , the result of equation (5):

$$\beta = 1.23$$

is very close to the results of FEM calculations given in [22]. For indenters with larger angles, equation (5) gives systematically lower values.

As mentioned above equation (3) is exact for cones but only a first order approximation for other geometries.

A similar correction should also be taken into account when trying to get the elastic penetration depth h_c under the contact area from unloading curves.

$$\frac{h_c}{D} = \frac{1 - \frac{1-2\nu}{4(1-\nu)} \cot \theta}{\frac{\pi}{2} - 0.883193 \frac{1-2\nu}{1-\nu} \cot \theta}$$

For a cube-corner and with $\nu=0$, this ratio is 0.54 instead of 0.637 the usual value for a cone neglecting the influence of radial displacements.

At this point the question arises to know if these corrections can be used for elastoplastic materials for which the initial surface is not flat but deformed by the plastic deformation. As previously established by Solomon [11], the problem can be solved by considering that the surface is deformed by an equivalent punch whose shape is defined by the distance between the indenter and the deformed surface. These equivalent indenters are best described by polynomials or power laws. For example the well-know Oliver and Pharr method [3] makes use of an equivalent indenters in the form of a paraboloid. To establish the corresponding corrections, analytical expressions for the radial displacements are needed.

It is possible to simply derive such expressions from Sneddon's equations.

In cylindrical coordinates and using Hankel's transform [19], the biharmonic equilibrium equation can be expressed on the undeformed surface by the following set of integral equations:

$$\begin{aligned} u_r(r, z) &= \frac{\lambda + \mu}{\mu} \int_0^\infty \xi^2 \frac{\partial G}{\partial z} J_1(\xi r) d\xi \\ u_z(r, z) &= \int_0^\infty \xi \left(\frac{\partial^2 G}{\partial z^2} - \frac{\lambda + 2\mu}{\mu} \xi^2 G \right) J_0(\xi r) d\xi \\ \tau_{rz}(r, z) &= \int_0^\infty \xi^2 \left[\lambda \frac{\partial^2 G}{\partial z^2} + (\lambda + 2\mu) \xi^2 G \right] J_1(\xi r) d\xi \\ \sigma_{zz}(r, z) &= \int_0^\infty \xi \left[(\lambda + 2\mu) \frac{\partial^3 G}{\partial z^3} - (3\lambda + 4\mu) \xi^2 \frac{\partial G}{\partial z} \right] J_0(\xi r) d\xi \end{aligned}$$

z and r are cylindrical coordinates respectively normal and parallel to the surface, $u_r(r, z)$ and $u_z(r, z)$ the radial and normal displacements, $\tau_{rz}(r, z)$ the shear stress and $\sigma_{zz}(r, z)$ the normal stress.

$J_0(\xi r)$ and $J_1(\xi r)$ are Bessel functions of the first kind.

$G(\xi, z) = [C(\xi) + zD(\xi)]e^{-\xi z}$ is a function vanishing far from the surface and satisfying the boundary conditions.

For a frictionless punch ($\tau_{rz} = 0$), with: $\rho = \frac{r}{a}$ and $\xi = \frac{t}{a}$, the integral equations can be written at the surface for $z=0$, and for the contact radius a :

$$\begin{aligned} \sigma(\rho) &= 2(\lambda + \mu) \int_0^\infty t g(t) J_0(\rho t) dt & 1 < \rho < \infty \\ w(\rho) &= -\frac{a(\lambda + 2\mu)}{\mu} \int_0^\infty g(t) J_0(\rho t) dt & \rho < 1 \\ u(\rho) &= a \int_0^\infty g(t) J_1(\rho t) dt & \rho < 1 \end{aligned} \quad (6)$$

Applying the inverse Hankel's transform and since $\sigma(\rho)=0$ for $\rho>1$:

$$g(t) = \frac{1}{2(\lambda + \mu)} \int_0^1 \rho \sigma(\rho) J_0(\rho t) d\rho$$

and replacing $g(t)$ by this value:

$$w(z) = -\frac{a(\lambda + 2\mu)}{2\mu(\lambda + \mu)} \int_0^1 \rho \sigma(\rho) d\rho \int_0^\infty J_0(\rho t) J_0(z t) dt$$

$$u(z) = \frac{a}{2(\lambda + \mu)} \int_0^1 \rho \sigma(\rho) d\rho \int_0^\infty J_0(\rho t) J_1(z t) dt$$

Using elementary properties of Bessel functions:

$$\int_0^\infty J_0(\rho t) J_0(z t) dt = \frac{2}{\pi} \int_0^{\min(z, \rho)} \frac{dx}{\sqrt{(\rho^2 - x^2)(z^2 - x^2)}} \quad (6)$$

$$\int_0^\infty J_0(\rho t) J_1(z t) dt = \begin{cases} 0, & z < \rho \\ \frac{1}{z}, & z > \rho \end{cases} \quad (7)$$

The normal displacements can be written:

$$w(z) = -\frac{2}{\pi} \frac{a(\lambda + 2\mu)}{2\mu(\lambda + \mu)} \int_0^z \frac{dx}{\sqrt{z^2 - x^2}} \int_x^1 \frac{\rho \sigma(\rho) d\rho}{\sqrt{\rho^2 - x^2}}$$

the stress distribution being obtained inverting Abel's integrals:

$$F(x) = \frac{2}{\pi} \int_0^x \frac{z w(z) dz}{\sqrt{x^2 - z^2}}$$

$$\sigma(\rho) = -\frac{2}{\pi} \frac{d}{d\rho} \int_\rho^1 \frac{x F(x) dx}{\sqrt{x^2 - \rho^2}}$$

or [23]:

$$\sigma(\rho) = \frac{4a\mu(\lambda + \mu)}{\pi a(\lambda + 2\mu)} \int_\rho^1 \frac{F'(x) dx}{\sqrt{x^2 - \rho^2}}$$

An important expression for the radial displacements is also obtained from equation (7), once the normal stress has been calculated:

$$u(\rho) = \frac{a}{2(\lambda + \mu)} \frac{1}{\rho} \int_0^\rho z \sigma(z) dz \quad (8)$$

Incidentally, equation (8) shows that the only solution for a frictionless punch to give identical initial and final contact areas is the trivial solution: $P=0$.

With these results the solution of equation (3) is the solution of the integral equation:

$$-\frac{2}{\pi} \frac{a(\lambda + 2\mu)}{2\mu(\lambda + \mu)} \int_0^z \frac{dx}{\sqrt{z^2 - x^2}} \int_x^1 \frac{\rho \sigma(\rho) d\rho}{\sqrt{\rho^2 - x^2}} + \frac{a \cot \theta}{2(\lambda + \mu)} \frac{1}{\rho} \int_0^\rho z \sigma(z) dz = w(z)$$

$w(z)$ describing the shape of the indenter.

This equation could be solved by using for example an iteration method.

For an indenter in the form of a paraboloid:

$$w(z) = D - k a^2 z^2$$

with:

$$\sigma(\rho) = -\frac{16\mu(\lambda + \mu)}{\pi(\lambda + 2\mu)} a k \sqrt{1 - \rho^2}$$

$$u(\rho) = -\frac{8\mu}{3(\lambda + 2\mu)} k a^2 \frac{1 - (1 - \rho^2)^{\frac{3}{2}}}{\rho}$$

In the more general case of an indenter obeying a power law, the exponent being or not an integer:

$$f(\rho) = c_n a^n z^n$$

$$\sigma(\rho) = -\frac{2\mu(\lambda + \mu)}{\lambda + 2\mu} c_n a^{n-1} \frac{n \Gamma(\frac{n}{2})}{\Gamma(\frac{1+n}{2})} \left[\frac{n}{\sqrt{\pi(n-1)}} {}_2F_1\left(\frac{1}{2}, \frac{1-n}{2}; \frac{3-n}{2}; \rho^2\right) - \frac{n \Gamma(\frac{1-n}{2})}{\Gamma(-\frac{n}{2})} \rho^{n-1} \right] \quad (9)$$

$$u(\rho) = \frac{\mu}{\sqrt{\pi(\lambda + 2\mu)}} \frac{n^2 \Gamma(\frac{n}{2})}{(n+1) \Gamma(\frac{1+n}{2})} c_n a^n \left[\frac{\sqrt{\pi} \Gamma(\frac{1-n}{2})}{n \Gamma(-\frac{n}{2})} \rho^n - \frac{1 - \sqrt{1-\rho^2}}{\rho} - \frac{\rho}{n-1} {}_2F_1\left(\frac{1-n}{2}, \frac{1}{2}; \frac{3-n}{2}; \rho^2\right) \right] \quad (10)$$

Where ${}_2F_1(a,b;c;d)$ is the Gauss hypergeometric function easily calculated with mathematical packages as for example Mathematica (Wolfram Research). When n is an odd integer these expressions are indeterminate, but in that case Sneddon [23] indicated how to obtain $\sigma(\rho)$. His results will be reviewed since they contain several typing errors.

$$\sigma(\rho) = \frac{4\mu(\lambda + \mu)}{\sqrt{\pi(\lambda + 2\mu)}} \frac{n \Gamma(1 + \frac{n}{2})}{\Gamma(\frac{1}{2} + \frac{n}{2})} a^{n-1} i_n(\rho)$$

the i_n functions being calculated by a recursion relation:

$$i_n = \frac{\sqrt{1-\rho^2}}{n-1} + \frac{n-2}{n-1} \rho^2 i_{n-2}$$

The expressions for $\sigma(\rho)$ and $u(\rho)$, for n between 1 and 10, are listed in the Appendix because they can be useful for practical purposes. The corresponding expressions for the radial displacements are obtained from equation (8).

As mentioned above, expressions (9) and (10) are undetermined and the iterative solution proposed by Sneddon should be used [23]. However, the general formulas (9) and (10) can still be used since correct values are obtained as the limits of the formula when the exponent n tends to an odd integer. For example for $n=1.0000001$ the first 7 digits are correct.

The β parameter for the parabolic punch ($n=2$) can thus be calculated from the approximate equation (3):

$$f(\rho) = ka^2 \left(\rho - \frac{16\mu(\lambda + \mu)}{\pi(\lambda + 2\mu)} a k [1 - (1-\rho^2)^{\frac{3}{2}}] \right)^2$$

giving:

$$\beta = \frac{1 - 2.54648a k \frac{1-2\nu}{2(1-\nu)} + 0.169459 [a k \frac{1-2\nu}{2(1-\nu)}]^2}{1 - 3.81972a k \frac{1-2\nu}{2(1-\nu)} + 1.3469 [a k \frac{1-2\nu}{2(1-\nu)}]^2} \quad (11)$$

The dimensionless parameter ak

$$ak = \frac{D}{2a}$$

is related to the radius of curvature R of the paraboloid:

$$ak = \frac{1}{2R}$$

In a material exhibiting a large plasticity and since it contributes only to a correction factor, it can be taken as

$$ak = \frac{h_e}{a}$$

with h_e the elastic deformation and h_t the total penetration depth.

For a Berkovich indenter it comes:

$$a_k = \frac{\sqrt{\pi}}{\sqrt{24.56}} \frac{h_c}{h_t}$$

For an equivalent indenter described by a power law with a non integer exponent, it is possible to expand in powers the quantity:

$$\left(1 - \frac{u(\rho)}{\rho}\right)^n$$

and perform the numerical integrations on the retained terms.

Experimentally in an elastic material, where the correction for a cone is supposed to apply, the variations of β should be observable when using indenters with different angles. From equation (5), a ratio of 1.083 should be observed with $\nu=0.3$, between a Berkovich indenter and a cube-corner. On the contrary, in a material exhibiting a large plasticity with a low h_c/h_t and taking a paraboloid as equivalent indenter, the correction should be small and probably negligible. This last point will be verified experimentally.

EXPERIMENTAL

Preliminary experimental work was done using a NHT nanoindentation apparatus and a specially designed indenter both from CSM Instruments (Peseux Switzerland). The tip was not designed for this purpose but rather to allow direct contact area determination even in cases where pile-up or sinking-in occurs. The tip consists, as shown in figure 2, in a cube-corner terminated by a small Berkovich part.

Multicycle experiments, shown in figure 3, were performed in a copper specimen, a plastic material. Two regimes are visible on this figure. The first one at low penetration depths corresponding to the Berkovich part of the tip and the second one, at larger penetration, corresponding to the cube-corner. Stiffness measured at the end of each cycle is plotted in figure 4 versus the maximum penetration depth. This plot exhibits an abrupt transition between the two regimes. The contact area is known at this point provided that the normal cross section of the indenter at the transition was previously measured, for example by Atomic Force Microscopy or Scanning Electron Microscopy. Thus the contact area is precisely known at the transition between the two parts of indenter independently of the presence, or not, of pile-up or sinking-in. It is thus possible to derive at this point reliable values for the elastic modulus and the hardness.

In figure 5, the inverse stiffness is plotted versus $F^{-1/2}$ and no transition can be observed. For a given bulk material and at sufficient penetration depths, the elastic modulus and the hardness are assumed to be constant and the slopes of the two segments of the curve depend only on the β parameters associated with the Berkovich and the cube-corner parts of the indenter.

Adopting the β parameters given by equation (5) for a conical tip, the slopes should be in a ratio of 1.083 easily visible on the curves. An even larger ratio would be observed using equation (4). Actually, since the β parameters seem to be equal, the situation is best described by assuming for unloading an equivalent indenter in the form of a paraboloid, as in the Oliver and Pharr method. On figure 3 it is apparent that the values of the ratio h_c/h_t are very low, corresponding to a large radius of curvature for the equivalent indenter and leading to corrections quite negligible, as seen before. When plasticity develops progressively in a material, the exponent of the equivalent indenter starts from 1 (cone) and goes progressively to larger values.

1
2
3 With the above indenter geometry the contact area can be determined for all penetration depths only
4 when the elastic modulus, or the hardness, doesn't change with this penetration depth. The curve in
5 Figure 4 being made, as shown above, of two straight segments. In cases where the elastic modulus is
6 not constant, for example in coated materials, a different indenter whose shape is shown in Figure 6
7 (patent pending) must be used. With this indenter the area at the transition can be freely adjusted by
8 slightly modifying the orientation of the sample surface relative to the indentation direction.

9
10 With this indenter the transition occurs for the penetration depth h_0 :

$$11 \quad h_0 = h \cos \alpha$$

12 h is the displacement in the indentation direction and α the angle between the indenter and the
13 indentation direction. The contact area A at this transition is:

$$14 \quad A = \frac{A_0}{\cos \alpha}$$

15 with A_0 the surface of the flat extremity of the indenter normal to the indentation direction as shown in
16 Figure 6.
17

18 Theory, as well as experiments, concerning indentations not normal to the sample surface should be
19 developed.
20

21 **INFLUENCE OF SHEAR STRESSES.**

22 Indentations with sharp indenters are probably only poorly described by Sneddon's equations since
23 deformations can hardly be considered as infinitesimal and, for sharp indenters, the penetration is not
24 small compared to the radius of the contact area (Hertz conditions). Shear stresses have also to be
25 taken into account. These shear stresses may be due either to friction or simply to the fact that for a
26 frictionless indenter, stresses between the indenter and the material are normal to the interface with a
27 tangential component.

28 In both cases a set of two dual equations, corresponding to a mixed-mixed problem with unknown $g(t)$
29 and $h(t)$ has to be solved. This has been done by several authors [24] [25] [26].
30

31 In the case of full adhesion, $u(\rho)=0$ for $\rho<1$, exact solutions are available [24]:
32 for the adhesive circular flat punch:

$$33 \quad \beta = \frac{1-\nu}{1-2\nu} \text{Log}(3-4\nu) \quad \beta=1.096 \quad (\nu=0)$$

34 and for the adhesive cone:

$$35 \quad \beta = \frac{2(1-\nu)}{\sqrt{3-4\nu}} \quad \beta=1.1547 \quad (\nu=0.)$$

36 For an adhesive sphere, no analytical solution have been proposed but Spence [24] computed
37 numerically β parameters for different values of ν . For example $\beta=1.196$ for $\nu=0$.
38

39 For a pyramidal indenter one has also to take into account the β value computed above for triangular
40 and square cross sections, respectively 1.064 and 1.021.
41

42 In practical cases friction or full adhesion may extend to the whole contact area or only to a portion of
43 it. The corresponding values of β are not easily determined since the friction coefficient and the
44 concerned portions of the contact area are usually not precisely known.
45

46 **CONCLUSION**

47 The problem of the determination of the elastic compliance during indentation of an elastic half plane
48 by a non axisymmetric frictionless punch was examined. A general formula for cross sections in the
49
50
51
52
53
54
55
56
57
58
59
60

form of regular polygons has been proposed. For square or triangular cross section, precise values of the β parameter were obtained, respectively 1.02121 and 1.06142.

General expressions relating to the distribution of normal stresses and radial displacements, for real or equivalent indenters obeying polynomial or power laws have been proposed. β values taking into account radial displacements have also been discussed for cones or paraboloids. These results seem to indicate that corrections for the β parameter can be ignored for materials with a large plasticity.

Finally preliminary results obtained with specially designed indenters eliminating uncertainties in the determination of the contact area in the presence of pile-up or sinking-in, have been presented.

APPENDIX

The values of $\sigma(\rho)$ and $u(\rho)$ listed below must be multiplied by the factors k_n and l_n respectively:

$$k_n = \frac{4\mu(\lambda + \mu)}{\lambda + 2\mu} \frac{n \Gamma(1 + \frac{n}{2})}{\sqrt{\pi} \Gamma(\frac{1}{2} + \frac{n}{2})}$$

$$l_n = \frac{2\mu a}{\lambda + 2\mu} \frac{n \Gamma(1 + \frac{n}{2})}{\sqrt{\pi} \Gamma(\frac{1}{2} + \frac{n}{2})}$$

n=1

$$\sigma(\rho) = \text{ArcSech}(\rho)$$

$$u(\rho) = \frac{1 - \sqrt{1 - \rho^2} + \rho^2 \text{ArcSech}(\rho)}{2\rho}$$

n=2

$$\sigma(\rho) = \sqrt{1 - \rho^2}$$

$$u(\rho) = \frac{1 - \sqrt{1 - \rho^2} (1 - \rho^2)}{3\rho}$$

n=3

$$\sigma(\rho) = \frac{1}{2} (\sqrt{1 - \rho^2} + \rho^2 \text{ArcSech}(\rho))$$

$$u(\rho) = \frac{6 - 4\sqrt{1 - \rho^2} + \sqrt{\frac{1 - \rho}{1 + \rho}} (-2 - 2\rho + 3\rho^2 + 3\rho^3) + 3\rho^4 \text{ArcSech}(\rho)}{24\rho}$$

n=4

$$\sigma(\rho) = \frac{1}{3} \sqrt{1 - \rho^2} (1 + 2\rho^2)$$

$$u(\rho) = \frac{3 + \sqrt{1 - \rho^2} (-3 + \rho^2 + 2\rho^4)}{15\rho}$$

n=5

$$\sigma(\rho) = \frac{1}{8} \sqrt{1 - \rho^2} (2 + 3\rho^2) + 3\rho^4 \text{ArcSech}(\rho)$$

$$u(\rho) = \frac{40 - 32\sqrt{1 - \rho^2} + \sqrt{\frac{1 - \rho}{1 + \rho}} (-8 - 8\rho + 10\rho^2 + 10\rho^3 + 15\rho^4 + 15\rho^5) + 15\rho^6 \text{ArcSech}(\rho)}{240\rho}$$

n=6

$$\sigma(\rho) = \frac{1}{15} \sqrt{1-\rho^2} (3+4\rho^2+8\rho^4)$$

$$u(\rho) = \frac{15 + \sqrt{1-\rho^2} (-15+3\rho^2+4\rho^4+8\rho^6)}{105\rho}$$

n=7

$$\sigma(\rho) = \frac{1}{48} \sqrt{1-\rho^2} (8+10\rho^2+15\rho^4) + 15\rho^6 \text{ArcSech}(\rho)$$

$$u(\rho) = \frac{336 - 288\sqrt{1-\rho^2} + \sqrt{\frac{1-\rho}{1+\rho}} (-48 - 48\rho + 56\rho^2 + 56\rho^3 + 70\rho^4 + 70\rho^5 + 105\rho^6 + 105\rho^7) + 105\rho^8 \text{ArcSech}(\rho)}{2688\rho}$$

n=8

$$\sigma(\rho) = \frac{1}{35} \sqrt{1-\rho^2} (5+6\rho^2+8\rho^4+16\rho^6)$$

$$u(\rho) = \frac{35 + \rho^2 \sqrt{1-\rho^2} (-35+5\rho^2+6\rho^4+8\rho^6+16\rho^8)}{315\rho}$$

n=9

$$\sigma(\rho) = \frac{1}{384} (\sqrt{1-\rho^2} (48+56\rho^2+70\rho^4+105\rho^6) + 105\rho^8 \text{Arc sec h}(\rho))$$

$$u(\rho) = \frac{1152 - 1024\sqrt{1-\rho^2} + \sqrt{\frac{1-\rho}{1+\rho}} (-128 - 128\rho + 144\rho^2 + 144\rho^3 + 168\rho^4 + 168\rho^5 + 210\rho^6 + 210\rho^7 + 315\rho^8 + 315\rho^9) + \frac{315\rho^{10} \text{ArcSech}(\rho)}{11520\rho}}{11520\rho}$$

n=10

$$\sigma(\rho) = \frac{1}{315} \sqrt{1-\rho^2} (35+40\rho^2+48\rho^4+64\rho^6+128\rho^8)$$

$$u(\rho) = \frac{315 + \sqrt{1-\rho^2} (-315+35\rho^2+40\rho^4+48\rho^6+64\rho^8+128\rho^{10})}{3465\rho}$$

REFERENCES

- [1] B.N. Lucas, W.C. Oliver and J.E. Swindeman, *Mat. Res. Soc. Symp. Proc.*, **522**, 3 (1998)
- [2] M.F. Doerner and W.D. Nix, *J. Mater. Res.*, **1**, 601 (1986)
- [3] W.C. Oliver and G.M. Pharr, *J. Mater. Res.*, **7**, 1564 (1992)
- [4] A. Bolshakov, W.C. Oliver and G.M. Pharr, *MRS Symp. Proc.* **356**, p 675 (1995).
- [5] J. Woiregard and J.C. Dargent, *J. Mater. Res.*, **12**, 2455 (1997)
- [6] S.I. Bulyshev, V.P. Alekhin, M.K. Shorshorov, A.P. Ternovskii and G.D. Shnyrev, *Zavod. La*, **41**, 1137 (1975).
- [7] G.M. Pharr, W.C. Oliver and F.R. Brotzen, *J. Mater. Res.*, **19**, 1, (1992).
- [8] R.T. Shield, *Z. Angew. Math. Phys.*, **18**, 682 (1967)
- [9] M.A. Jaswon and G.T. Symm, *Integral Equation Method in Potential Theory*, Academic Press London (1977)

- 1
2
3 [10] B. Nobble, *Conference on Applications of Numerical Analysis*. Ll. Morris, Ed. Springer Verlag,
4 Berlin (1971).
5 [11] S.K Laskar, *A Numerical Approach to Calculate Capacity of Conductors*, Department of
6 Mathematics, Assam Engineering College, Gauhati (1974)
7 [12] L. Solomon, *Elasticité Linéaire*, Masson Paris (1968)
8 [13] V.I. Fabrikant, *Int. J. Engng. Soc*, **24**, 1731 (1986)
9 [14] H. Motz, *Quart. Appl. Math.*, **4**, 371 (1946)
10 [15] R.B. King, *Int. J. Solids Structures* **23**, 1657 (1987)
11 [16] J.J. Vlassak and W.D. Nix, *J. Mech. Phys. Solids*, **42**, 1223 (1994)
12 [17] B.C. Hendrix, *J. Mater. Res.*, **10**, 255 (1995)
13 [18] A. Bolshakov and G.M. Pharr, *Mat. Res. Symp. Proc.*, Mat. Res. Soc., 189 (1997)
14 [19] I.N. Sneddon, *Fourier Transforms*, McGraw Hill, New York (1951)
15 [20] E.C. Titchmarsh, *Introduction to the Theory of Fourier Integrals*. Clarendon Press, Oxford (1937)
16 [21] I. W. Busbridge, *Proc. London Math. Soc.* **44**, 115 (1938)
17 [22] J. Hay, A. Bolshakov and G.M. Pharr, *J. Mater. Res.*, **14**, 2296 (1999)
18 [23] I.N. Sneddon, *Int. J. Engng. Sci.*, **3**, 47 (1965).
19 [24] D.A. Spence, *Proc. Roy. Soc.*, **A 305**, 55 (1968)
20 [25] L.A. Galin, *Contact Problems of the Theory of Elasticity and Viscoelasticity*, Nauka, Moscow
21 (1980)
22 [26] M. Barquins, *Wear*, **158**, 87 (1992).
23
24
25
26
27
28
29
30
31
32
33
34
35
36
37
38
39
40
41
42
43
44
45
46
47
48
49
50
51
52
53
54
55
56
57
58
59
60

FIGURES CAPTIONS**Figure 1**

Integration domain for a triangular indenter. The pressure distribution has only to be calculated in one of the six elementary triangles but the integration for the potential is extended to the whole domain.

Figure 2

Cube-corner/Berkovich composite indenter for the direct determination of the contact area at the penetration depth h_0 .

Figure 3

Multicycle indentation test with the cube-corne/Berkovich indenter on a Copper specimen. The two regimes are associated with the two parts of the indenter.

Figure 4

Elastic stiffness versus the maximum penetration depth in Copper, showing the transition between the cube corner and the Berkovich regimes. The contact area at this transition depends only of the the indenter geometry. An elastic modulus $E=120$ GPa, was measured.

Figure 5

Elastic compliance versus $F^{-1/2}$ in copper, showing that the β parameters are the same for the cube corner and the Berkovich parts of the indenter.

Figure 6

Prismatic indenter with two vertical faces and a triangular cross section for the determination of the contact area at the penetration depth $h_0=h \cos \alpha$.
 h is the displacement of the indenter parallel to the indentation direction and α the angle between the sample surface and the normal to the indentation direction.

1
2
3
4
5
6
7
8
9
10
11
12
13
14
15
16
17
18
19
20
21
22
23
24
25
26
27
28
29
30
31
32
33
34
35
36
37
38
39
40
41
42
43
44
45
46
47
48
49
50
51
52
53
54
55
56
57
58
59
60

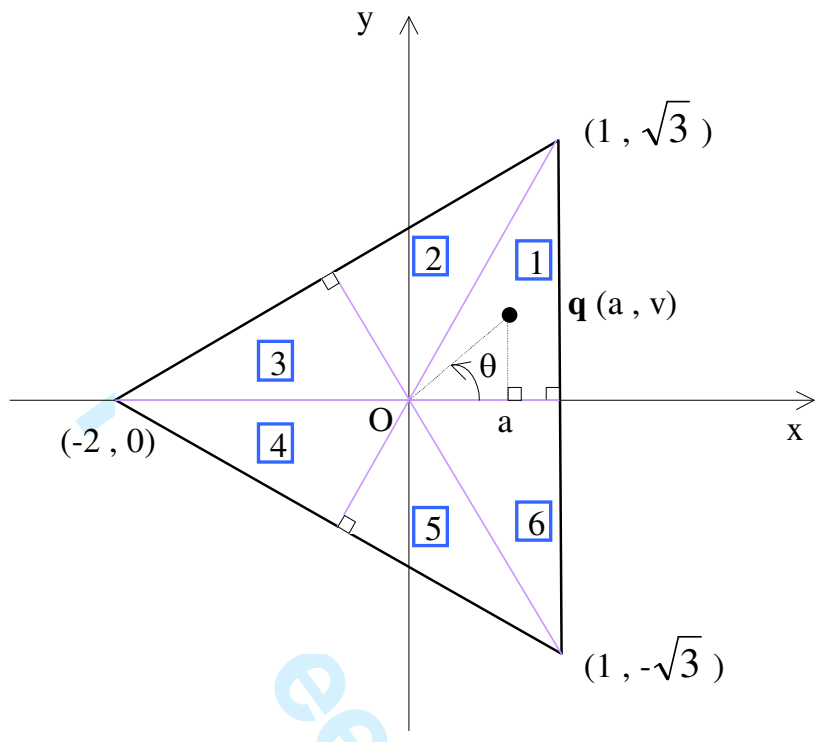


Figure 1

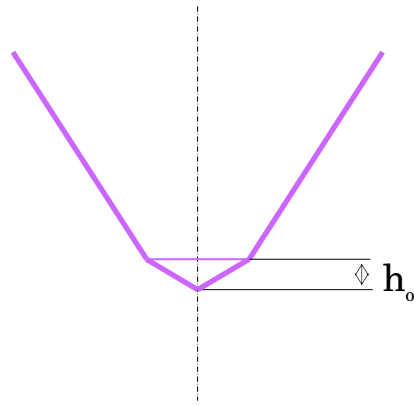


Figure 2

For Peer Review Only

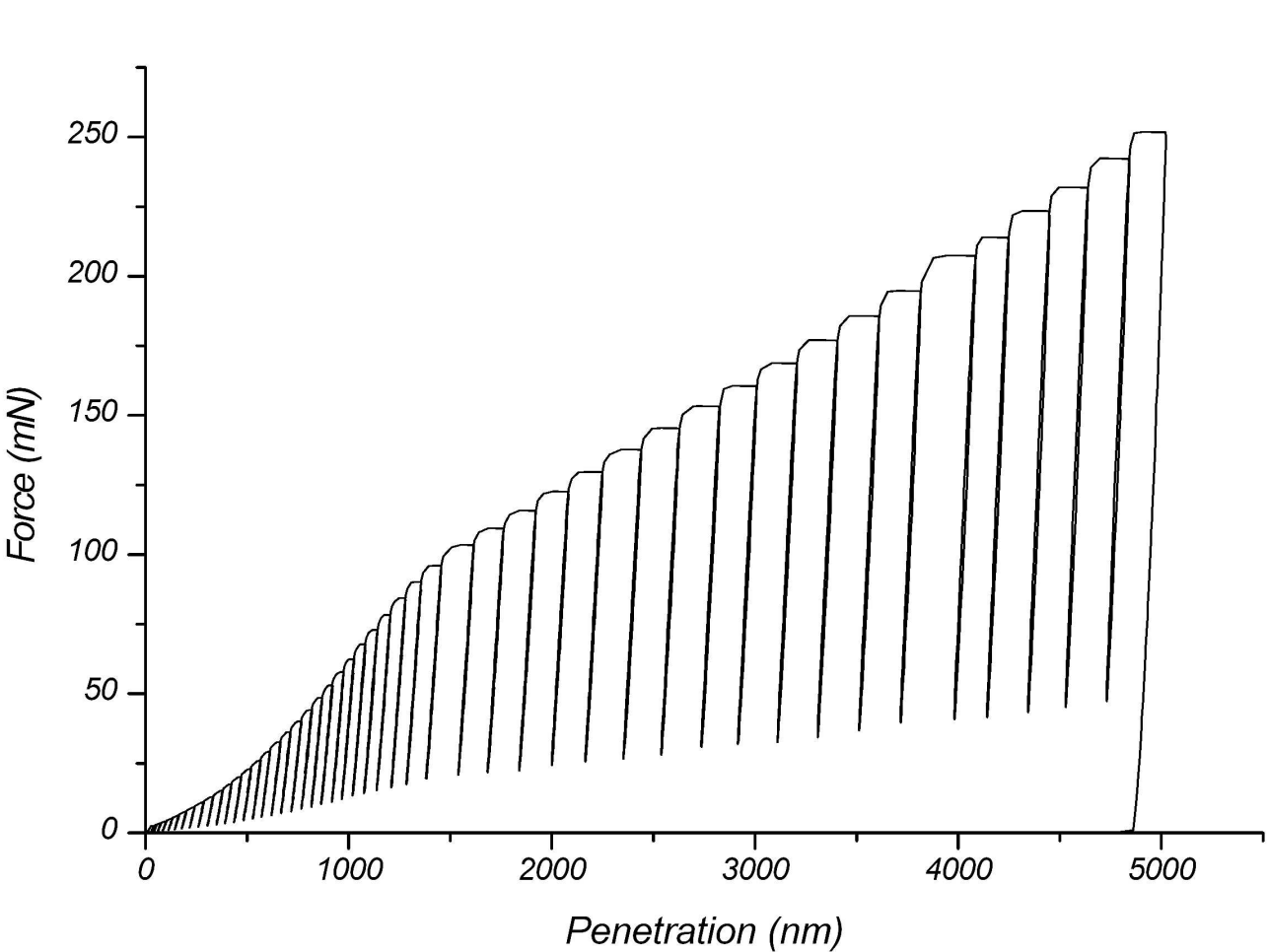


Figure 3

review Only

1
2
3
4
5
6
7
8
9
10
11
12
13
14
15
16
17
18
19
20
21
22
23
24
25
26
27
28
29
30
31
32
33
34
35
36
37
38
39
40
41
42
43
44
45
46
47
48
49
50
51
52
53
54
55
56
57
58
59
60

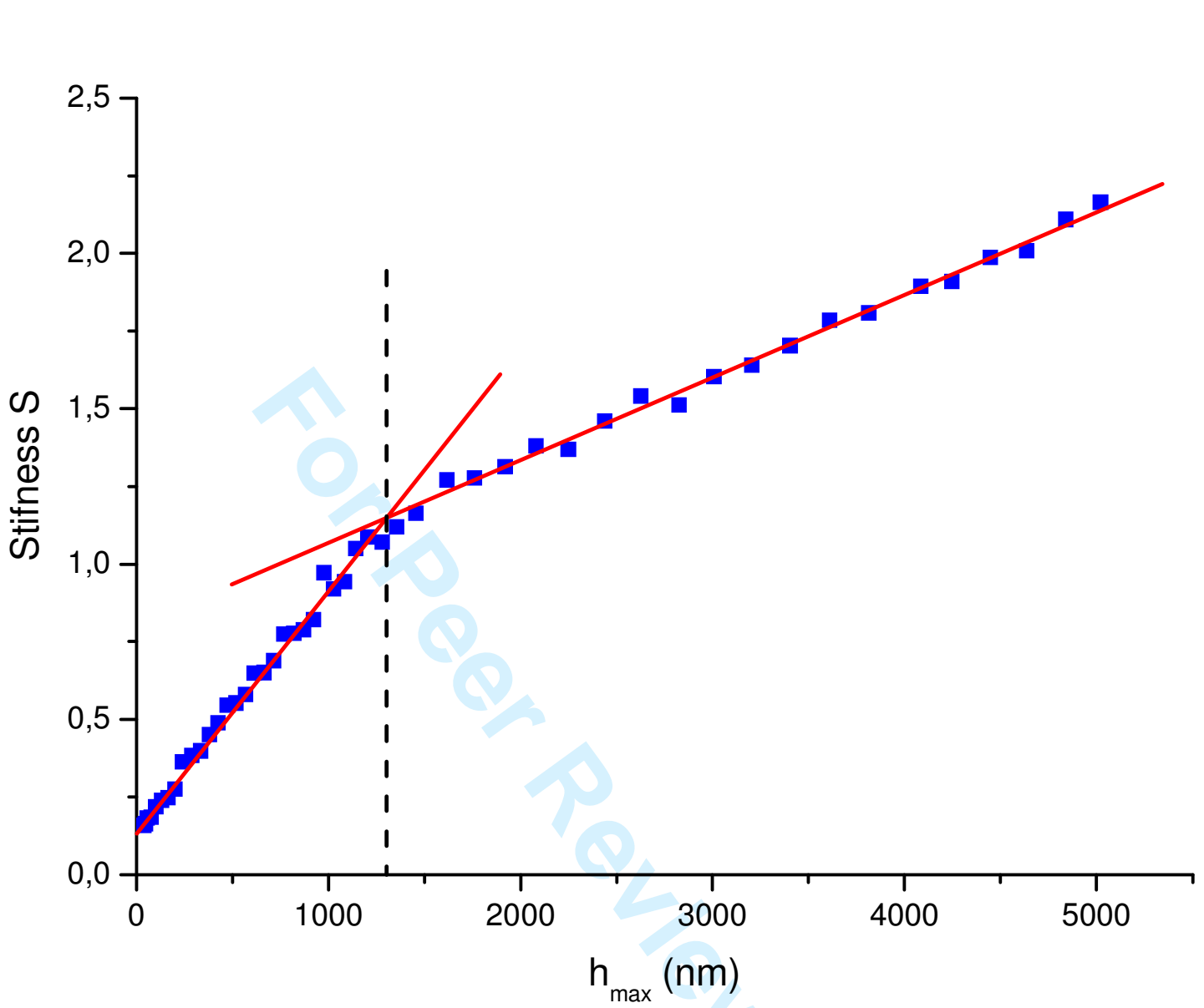


Figure 4

1
2
3
4
5
6
7
8
9
10
11
12
13
14
15
16
17
18
19
20
21
22
23
24
25
26
27
28
29
30
31
32
33
34
35
36
37
38
39
40
41
42
43
44
45
46
47
48
49
50
51
52
53
54
55
56
57
58
59
60

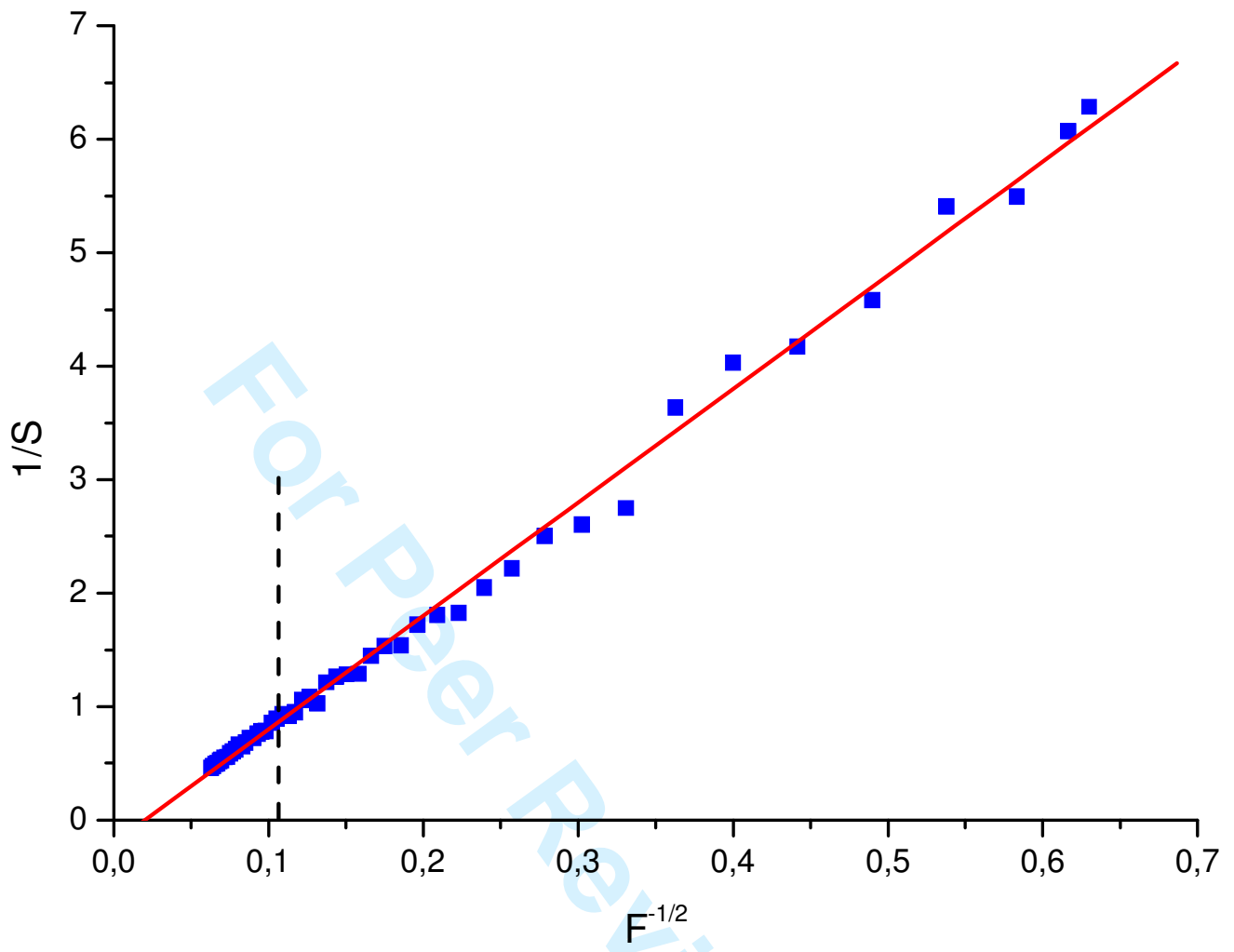


Figure 5

1
2
3
4
5
6
7
8
9
10
11
12
13
14
15
16
17
18
19
20
21
22
23
24
25
26
27
28
29
30
31
32
33
34
35
36
37
38
39
40
41
42
43
44
45
46
47
48
49
50
51
52
53
54
55
56
57
58
59
60

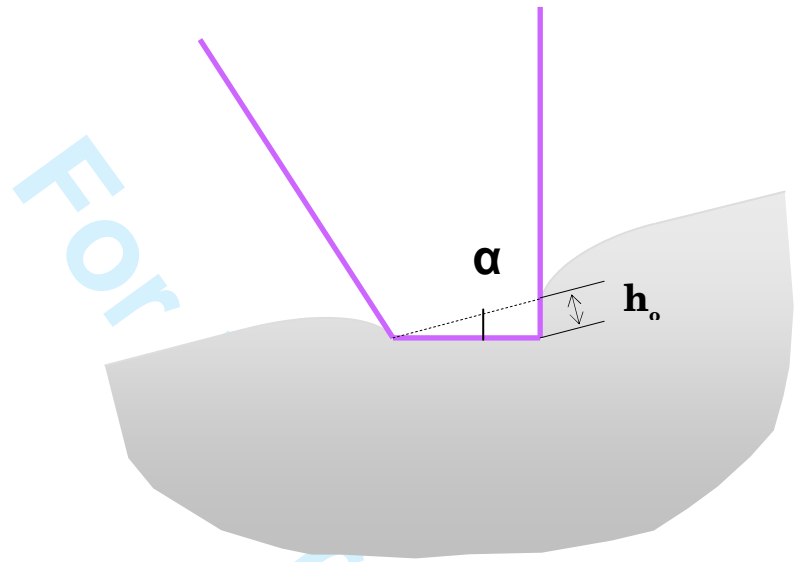


Figure 6